Journal of the Optical Society of America B
OPTICAL PHYSICS

Computation of the timing jitter, phase jitter, and linewidth of a similariton laser

JOHN ZWECK[1,*] AND CURTIS R. MENYUK[2]

[1]Department of Mathematical Sciences, The University of Texas at Dallas, Richardson, Texas 75080, USA
[2]Department of Computer Science and Electrical Engineering, The University of Maryland Baltimore County, Baltimore, Maryland 21250, USA
*Corresponding author: zweck@utdallas.edu

Received 26 December 2017; revised 27 March 2018; accepted 3 April 2018; posted 3 April 2018 (Doc. ID 318390); published 27 April 2018

We perform what we believe is the first computational study of phase jitter and comb linewidths in a nonsolitonic fiber laser with large changes in the pulse on each round trip. For fiber lasers operating in or near the similariton regime, we investigate how the pulse parameters and noise performance depend on the system parameters. Across a large dispersion range, the dechirped pulse width, timing jitter, phase jitter, and comb linewidths are smaller when the gain in the optical amplifier is larger. Over a narrow range of negative dispersion values near zero, the timing jitter and comb linewidths are smaller with a wider optical filter. However, with the wider optical filter, the pulse width increases significantly, and the noise performance deteriorates rapidly as the dispersion increases above zero. These trends are in general agreement with experimental studies of timing jitter and the linewidth of the carrier-envelope offset frequency in Yb-fiber lasers and are consistent with the Namiki–Haus theory of timing jitter in a stretched-pulse laser. © 2018 Optical Society of America

OCIS codes: (270.2500) Fluctuations, relaxations, and noise; (060.4370) Nonlinear optics, fibers; (140.3510) Lasers, fiber; (140.4050) Mode-locked lasers; (320.7090) Ultrafast lasers.

https://doi.org/10.1364/JOSAB.35.001200

1. INTRODUCTION

In this paper, we compute the width of a line in the frequency comb generated by a similariton laser due to amplified spontaneous emission (ASE) quantum noise, and we study the sensitivity of the linewidth to changes in the system parameters. Our approach is based on a formula for the power spectral density of the optical pulse train in terms of the power spectrum of the noise-free optical pulse, the timing jitter, and the phase jitter [1]. Since analytical expressions are not available for the timing jitter and the phase jitter, we use numerical methods to determine the periodically stationary noise-free pulse and to compute the timing and phase jitter.

By a similariton laser, we mean a laser that includes a normal dispersion fiber amplifier in which the pulse exiting the fiber amplifier has an approximately parabolic intensity and linear local frequency [2]. To obtain a periodically stationary pulse, these lasers typically also include a narrowband optical filter after the fiber amplifier [3]. Since the periodically stationary pulses in these lasers undergo large changes each round trip, their noise performance can be quite different from that predicted by models based on classical soliton perturbation theory, in which the pulse is assumed to be stationary [4–6]. For example, a computational simulation by Paschotta [5] showed that the power spectral density of the timing jitter of a particular similariton laser was substantially larger than what was predicted by a simple analytical model. The noise performance of similariton lasers must therefore be modeled using a computational method such as that of Paschotta [7,8], or the method we use here.

Fiber lasers designed to generate frequency combs typically consist of a mode-locked fiber laser, an external highly nonlinear fiber to facilitate the generation of an octave-spanning supercontinuum, and electronic feedback mechanisms to stabilize the comb. Newbury and Swann [9] describe a number of intracavity and extracavity noise sources that perturb the frequency comb. They argue that intracavity noise broadens the comb linewidths, while extracavity noise increases the noise floor.

Telle *et al.* [10] describe the fluctuations in a frequency comb due to system perturbations using the analogy of an elastic tape marked with equally spaced frequency lines that is held fixed at one point and randomly stretched due to the perturbations. Their model highlights the fundamental role that perturbations in the central time and phase of the pulse have on the uncertainty in the comb frequencies. The frequency of the nth line in the comb is given by $\nu_n = f_{\rm ceo} + nf_{\rm rep}$. In the presence of intracavity noise, the repetition frequency, $f_{\rm rep}$, and the carrier-envelope offset (ceo) frequency, $f_{\rm ceo}$, fluctuate on a time scale, T, that is slow compared to the round-trip time, resulting in a fluctuation, $\delta\nu_n(T)$, of the frequency of the nth line.

In their study of the frequency comb generated by a solitonic or stretched-pulse fiber laser, Newbury and Washburn [11] derived formulas for the perturbations in f_{ceo} and f_{rep} due to perturbations in the central time and phase of the pulse. They also derived a system of equations for the perturbations in the central time, phase, and other pulse parameters due to fluctuations in cavity length, gain and loss, and higher-order nonlinear and dispersive effects. However, they did not include perturbations due to ASE noise.

The power spectral density, $S_n(f)$, of the frequency noise on the nth comb line is the Fourier transform with respect to T of the frequency fluctuation, $\delta\nu_n(T)$. In the case of ASE noise, S_n is independent of f and the full width at half-maximum of the linewidth at optical frequency, ν_n, is $L_n = \pi S_n(0)$ [9]. Building on fundamental work of Haus and Mecozzi [4] for solitonic lasers, Paschotta and coworkers [5,7,8,12] and Menyuk and Wang [6] derived analytical formulas for the power spectral density of the frequency noise due to various quantum and technical noise perturbations. Their results were obtained for general-shaped stationary pulses but have also been applied to periodically stationary pulses with limited variations in the pulse parameters each round trip of the laser cavity. Based on the models of Paschotta, Newbury and Swann [9] calculated the contributions that the various noise sources make to the power spectral density of the frequency noise and hence to the linewidths, L_n. In particular, they showed that away from the center of the comb, the linewidth is dominated by the contribution due to pump-induced noise. However, analytical methods such as these are not valid for similariton lasers in which there are large changes in the pulse parameters each round trip.

Wahlstrand *et al.* [13] computed the optical comb linewidth as a function of frequency for a mode-locked Ti:sapphire laser using values of the phase and timing jitter obtained from experimentally derived parameters for the linear response of the laser to perturbations. More recently, Nugent-Glandorf *et al.* [14] measured the dependence of the linewidth of the ceo frequency, f_{ceo}, on the round-trip dispersion for a Yb-fiber laser without a narrowband optical filter. Since f_{ceo} is the product of the repetition rate and the carrier-envelope phase change per round trip, the linewidth of f_{ceo} is related to the timing jitter (due to noise on the repetition rate) and the phase jitter (due to noise on the carrier-envelope phase). For their system, the linewidth was minimized at zero dispersion, and increased more rapidly as the dispersion increased from zero than when it decreased from zero.

The idea for the similariton laser originated in the work of Fermann *et al.* [15], who found exact self-similar asymptotic solutions of the nonlinear Schrödinger equation in a fiber amplifier with normal dispersion and simple gain. They showed that after a sufficiently long propagation distance, an arbitrary pulse asymptotically evolves into a pulse with a parabolic power profile and a linear local frequency. The amplitude, pulse width, and spectral width of the asymptotic pulse increase exponentially with distance along the fiber and only depend on the energy of the input pulse. These similariton solutions therefore grow self-similarly in the fiber amplifier. However, the distance required before an initial pulse agrees with the asymptotic solution to within a specified tolerance depends on how closely the two solutions agree at the input. The existence of similaritons in a fiber amplifier led to the development of similariton lasers, which are based on two key ideas. The first key idea is that if the pulse entering the fiber amplifier is sufficiently close to the asymptotic solution, then it will rapidly converge to the asymptotic solution as it propagates through the fiber amplifier [15–17]. The existence of this attracting asymptotic solution thereby facilitates the formation of periodically stationary pulses. However, the parabolic pulse exiting the fiber amplifier is very far from the desired asymptotic solution at the entrance to the fiber amplifier. Therefore, in order to obtain a periodically stationary solution, the exiting pulse must be modified before re-entering the fiber amplifier. To achieve this goal, the second key idea is to insert a narrowband optical filter and a loss element after the fiber amplifier to ensure that the spectral width and energy of the pulse re-entering the fiber amplifier are sufficiently close to those of the asymptotic solution [18,19]. In addition to narrowing the pulse spectrum, since the local frequency of the pulse is linear in time, the optical filter also decreases the temporal width of the pulse to approximate that of the asymptotic solution. Chong *et al.* [3] showed that the key parameters affecting the shape of the pulses produced in the similariton laser are the nonlinearity, spectral bandwidth, and round-trip dispersion.

Taken together, a series of experimental studies [14,20–24] demonstrate that the design of similariton lasers can be further improved using a third key idea. For soliton and stretched-pulse lasers, the noise performance of the laser depends on the dispersion [4,25]. The idea is to insert a dispersive delay line into the loop to vary the round-trip dispersion. Since the asymptotic pulse only depends on the energy at the input to the fiber amplifier, the round-trip dispersion can be varied across a wide range from the normal to the anomalous dispersion regime without introducing large changes to the pulse at the exit to the fiber amplifier [20]. In this manner, it is possible to optimize the noise performance of the laser without introducing significant changes to the parameters of the pulse exiting the system.

In this paper, for a fiber laser with large changes in the pulse parameters each round trip, we systematically investigate how both the pulse parameters and the noise performance depend on the system parameters, and especially on the round-trip dispersion. The pulse parameters we consider are the energy, pulse width, peak power, chirp, and spectral width, and we quantify the noise performance in terms of the jitter in the energy, frequency, central time, phase of the pulse, and the width of the lines in the frequency comb. Our results are obtained for a fiber laser operating in or near the similariton regime. In addition to a baseline system whose design is close to that of several experimental systems [14,17,23], we consider two variants, a more nonlinear system with larger gain in the fiber amplifier, and a system with a wider optical filter. We show that the optimally compressed pulse width after the pulse exits the laser is smallest for the more nonlinear system and is insensitive to the round-trip dispersion. The width of the frequency comb is also largest for this system. Moreover, across the entire dispersion range we considered, the timing jitter, phase jitter,

and linewidths are also smaller for this variant of the system than for the baseline system. We also found that over a narrower range of negative dispersion values near zero, the timing jitter and comb linewidths are somewhat smaller for the system with the wider optical filter. However, with the wider optical filter, the pulse width increases significantly, and the noise performance deteriorates rapidly as the dispersion increases above zero. The trends that we report here are in general agreement with experimental studies of timing jitter [22,23] and the linewidth of the ceo frequency [14] in Yb-fiber lasers. To our knowledge, our work is the first computational study of phase jitter and the linewidth in a nonsolitonic fiber laser, and our results are consistent with trends observed in the Namiki–Haus theory of timing jitter in a stretched-pulse laser [25].

In Section 2, we describe our laser model, and in Section 3 we discuss the method that we used to compute the timing and phase jitter. In particular, we provide some theoretical justification for an intuitive method of McKinstrie and Xie [26] for computing phase jitter in a Monte Carlo simulation. In Section 4, we discuss the formulas we used for the power spectral density of the frequency comb and for the widths of the lines in the comb. We discuss numerical implementation issues in Section 5, and in Section 6 we present the results of our numerical simulations. In Section 7, we discuss relationships between our results and previous experimental and theoretical studies, and in Section 8 we present our conclusions and directions for future work.

2. LASER MODEL

We study mode-locked fiber laser systems in which an optical pulse is generated in a loop that consists of a nonlinear fiber amplifier, followed by a saturable absorber, an optical filter, a dispersive delay line, and an output coupler. After the optical pulse exits the loop, it is compressed by an external dispersive delay line to obtain the minimum possible pulse width. The system parameters can be chosen so that this simplified laser system is similar to several experimental Yb-fiber laser combs that operate in the stretched-pulse or similariton regimes [2,14,16,17,19–21,23,27–29]. Because of the large changes in the pulse parameters each round trip, an averaged (or distributed) laser model is not appropriate. Instead, we use a full (or lumped) laser model in which we model the action of each laser component on the light as it passes through that component [6].

We model the fiber amplifier using the nonlinear Schrödinger equation with band-limited saturable gain,

$$\frac{\partial u}{\partial z} = \left[\frac{g}{2}\left(1 + \frac{1}{\Omega_g^2}\frac{\partial^2}{\partial t^2}\right) - i\frac{\beta}{2}\frac{\partial^2}{\partial t^2} + i\gamma|u|^2\right]u. \tag{1}$$

Here $u = u(z,t)$ is the electric field envelope of the light, where z denotes position in the fiber amplifier, and t is retarded time across the pulse. The saturable gain, g, is given by

$$g(z) = \frac{g_0}{1 + E(z)/E_{\text{sat}}}, \tag{2}$$

where g_0 is the unsaturated gain, $E(z)$ is the pulse energy at position z, and E_{sat} is the saturation energy. For simplicity, in Eq. (1) we model the finite bandwidth of the amplifier using a Gaussian filter with bandwidth Ω_g. For simulations with noise, we add white Gaussian noise in the fiber amplifier. The chromatic dispersion coefficient, β, is negative in the anomalous dispersion regime and positive in the normal dispersion regime, and the γ is the nonlinear Kerr coefficient of the fiber. We model the saturable absorber using the fast saturable loss transfer function

$$u_{\text{out}} = \left[1 - \frac{l_0}{1 + |u_{\text{in}}|^2/P_{\text{sat}}}\right]u_{\text{in}}, \tag{3}$$

where l_0 is the unsaturated loss and P_{sat} is the saturation power. We model the optical filter as a Gaussian filter, which typically has a much narrower bandwidth than that of the fiber amplifier.

3. TIMING AND PHASE JITTER

In this section, we discuss the method we used to compute the timing and phase jitter in a mode-locked laser, and in the next section, we will use the computed timing and phase jitter in a formula for the width of a comb line. For the laser systems we studied, the variances of the timing and phase shifts are linear functions of the number of round trips of the laser. We therefore define the timing and phase jitter per round trip to be the square root of the timing and phase variance per round trip. To calculate the timing and phase variances, we need definitions for the timing and phase shifts of a pulse due to noise perturbations.

Following standard practice [30], we define the central time, t_C, of an optical pulse, u, using the moment integral

$$t_C = \frac{\int_{-\infty}^{\infty} t|u(t)|^2 \mathrm{d}t}{\int_{-\infty}^{\infty} |u(t)|^2 \mathrm{d}t}, \tag{4}$$

and the timing shift, Δt, of a noise-perturbed pulse to be the amount that t_C changes due to the perturbation. In situations where it is applicable, perturbation theory can be used to provide an alternate definition of the timing shift. Specifically, in the existing perturbation theories for soliton and stretched-pulse lasers [4,25], the noise-perturbed optical pulse is given in terms of several pulse parameters, including the central time and phase. In this situation, the timing shift is defined to be the shift in the time parameter due to the perturbation. An evolution equation for the timing shift is then derived by taking an inner product between the noise-perturbed pulse and the dual of the timing mode of the linearization of the governing equation. Significantly, these two definitions of the timing shift agree: Menyuk and Wang [6] proved that the timing shift obtained from perturbation theory is equal to that obtained from Eq. (4).

However, unlike the case of the timing shift, there is no universally agreed-upon definition for the phase shift, and there can be a lack of agreement between the phase shifts computed using the different definitions in the literature. For example, in situations where soliton perturbation theory is applicable, the phase shift obtained from the projection of the noise-perturbed pulse onto the phase mode of the linearized equation is not consistent with intuitive definitions of the phase shift, such as the definition of McKinstrie and Xie we discuss below [26]. This lack of agreement has implications for the quantitative application of perturbation theories to the noise

performance of mode-locked lasers and is a topic that merits further investigation. Specifically, in their study of the phase jitter in a soliton-based optical communications system, McKinstrie and Xie [26] introduced two methods to numerically compute the phase shift of a noise-perturbed pulse in a Monte Carlo simulation. In the first method, they define the phase of the pulse in terms of moment integrals for the real and imaginary parts of the complex field envelope. This definition, which forms the basis of the method that we will use for the results in this paper, is given below. In the second method, after filtering out high-frequency noise, they define the phase of the pulse to be the time average of the instantaneous phase. Using Monte Carlo simulations, they showed (and we verified) that although the phase jitters computed using these two methods agree, they are both significantly different from the formula for the phase jitter derived by Iannone *et al.* [31] using soliton perturbation theory. In soliton perturbation theory, any function can be decomposed as a linear combination of four discrete modes (timing, phase, amplitude, and frequency) and the continuum. Based on results of Moore *et al.* [32], we suggest that the lack of agreement observed by McKinstrie and Xie occurs not because of a breakdown in soliton perturbation theory, but because the phase shifts computed using the two numerical methods of McKinstrie and Xie are influenced, not only by the projection onto the phase mode, but also by contributions from the continuum. To circumvent this problem, for the important sampling method they developed, Moore *et al.* [32] computed the phase shift of a noise-perturbed pulse by numerically projecting the pulse onto the phase eigenfunction of the linearized system. However, such an approach is only available for laser systems for which there is a well-established perturbation theory, either analytical or computational in nature [6], and it is an open question as to whether such a definition of the phase shift is relevant for the computation of comb linewidths in an experimental system. Moreover, since we are not aware of any published work on a perturbation theory for similariton lasers, it is not currently possible to define the phase shift for a pulse in a similariton laser using the method of Moore *et al.* Therefore, for the results in this paper, we define the phase shift using a modification of the first method of McKinstrie and Xie, which, as we will show, is appropriate for use in the formula that we will derive in the next section for the width of a comb line.

We assume that, in the absence of noise, after the nth round trip of the laser, the output optical pulse is of the form

$$u_n(t) = U(t - nT_R)\exp(in\phi_{\mathrm{sl}}), \quad \text{where}$$
$$U(t) = \sqrt{E}R(t)\exp[-i\phi(t)]. \tag{5}$$

Here E is the pulse energy, and R is a real-valued function normalized so that $\int_{-\infty}^{\infty}|R(t)|^2\mathrm{d}t = 1$. The parameter T_R is the round-trip time, and ϕ_{sl} is the phase slip from one round trip to the next. We assume that the phase function, ϕ, is of the form

$$\phi(t) = \phi_c + \omega_c t + Ct^2. \tag{6}$$

To first order, the effect that noise has on the pulse, u, is to shift the energy, central time, phase, and central frequency of the pulse. In addition, a continuum contribution is generated. In contrast to the case of soliton perturbation theory, here we simply assume that in the presence of noise, after the nth round trip, the pulse exiting the loop at the output coupler is of the form

$$u_n(t) = (1 + \Delta E_n/E)^{1/2}U(t - nT_R - \Delta t_n) \times \exp[i(n\phi_{\mathrm{sl}} + \Delta\theta_n + \Delta\omega_n(t - nT_R))], \tag{7}$$

for some random shifts ΔE_n, Δt_n, $\Delta\theta_n$, and $\Delta\omega_n$. However, we ignore any radiation. We can compute ΔE_n, Δt_n, and $\Delta\omega_n$ using moment integrals of the perturbed pulse, u_n [30].

We will now show that a slight modification of the first method of McKinstrie and Xie can be used to compute the phase shift, $\Delta\theta_n$. Simplifying notation and transforming to local time, we seek to extract the phase-shift parameter, $\Delta\theta$, from a noise-perturbed pulse of the form

$$u(t) = (1 + \Delta E/E)^{1/2}U(t - \Delta t)\exp[i(\psi_{\mathrm{sl}} + \Delta\theta + \Delta\omega t)], \tag{8}$$

given that ΔE, Δt, and $\Delta\omega$ have already been computed. To that end, we first shift the frequency of u by $\Delta\omega$ and then shift the resulting pulse in time by Δt to obtain

$$v(t) = u(t + \Delta t)\exp[-i\Delta\omega(t + \Delta t)] = (1 + \Delta E/E)^{1/2}U(t)\exp[i(\psi_{\mathrm{sl}} + \Delta\theta)]. \tag{9}$$

Next, we compute the moment integrals

$$X = \int_{-\infty}^{\infty}\Re(v)|v|^2\mathrm{d}t \quad \text{and} \quad Y = \int_{-\infty}^{\infty}\Im(v)|v|^2\mathrm{d}t, \tag{10}$$

and set $\psi = \arg(X + iY)$. A calculation using trigonometric addition formulas then shows that

$$\Delta\theta = \psi - \arg(C_U + iS_U) - \psi_{\mathrm{sl}}, \tag{11}$$

where

$$C_U = \int_{-\infty}^{\infty}\Re(U)|U|^2\mathrm{d}t \quad \text{and} \quad S_U = \int_{-\infty}^{\infty}\Im(U)|U|^2\mathrm{d}t. \tag{12}$$

Since the parameters C_U, S_U, and ψ_{sl} do not depend on the noise, the phase variance is given by $\mathbb{E}[(\Delta\theta - \mathbb{E}[\Delta\theta])^2] = \mathbb{E}[\psi^2]$, which can be computed using a Monte Carlo simulation.

4. COMB LINEWIDTHS

In this section, we compute the power spectral density of the frequency comb generated by a mode-locked laser and the linewidth of a comb line. Here, we summarize the derivation of the formulas that we use to relate these quantities to phase and timing jitter. More details may be found in [1]. For this calculation we assume that the width of a comb line depends primarily on the timing variance, phase variance, and time-phase covariance.

By Eq. (7), the output optical pulse train is of the form

$$u(t) = \sum_{n=-\infty}^{\infty}A_nU(t - nT_R - \Delta t_n)\exp[i\Delta\phi_n(t - nT_R)], \tag{13}$$

where $A_n = (1 + \Delta E_n/E)^{1/2}$ and $\Delta\phi_n(t) = n\phi_{\mathrm{sl}} + \Delta\theta_n + \Delta\omega_n t$. The power spectral density of the stationary process, u, is given by

$$S(\omega) = \lim_{T\to\infty} \mathbb{E}[|\widehat{u}_T(\omega)|^2], \tag{14}$$

where $\mathbb{E}$ is the expectation operator, and

$$\widehat{u}_T(\omega) = \frac{1}{\sqrt{2T}} \int_{-T}^{T} u(t) \exp(-i\omega t) \mathrm{d}t. \tag{15}$$

A calculation shows that [1]

$$S(\omega) = \frac{1}{T_R} \sum_{n=-\infty}^{\infty} \mathbb{E}[A_o A_n \exp\{i(\Delta\theta_0 - \Delta\theta_n + \omega(\Delta t_n - \Delta t_0))\} \times \exp\{in(T_R\omega - \phi_{sl})\} \widehat{U}(\omega - \Delta\omega_0) \widehat{U}^*(\omega - \Delta\omega_n)]. \tag{16}$$

In Section 6, we will describe results of numerical simulations of a similariton laser, which show that while the variances of the timing and phase shifts grow linearly with the number of round trips, the variances of the energy and frequency shifts are small and essentially constant as a function of the number of round trips of the laser. The reason for this behavior is that the gain saturation of the fiber amplifier and the optical filter in the loop stabilize the pulse energy and central frequency, respectively. These results suggest that it is reasonable to assume that the energy and central frequency perturbations in Eq. (16) are zero, i.e., that $A_0 = A_n = A$ and $\Delta\omega_0 = \Delta\omega_n = 0$ for all n. Consequently, we obtain

$$S(\omega) = \frac{E}{T_R} |\widehat{U}(\omega)|^2 \sum_{n=-\infty}^{\infty} \mathbb{E}[\exp\{i(\Delta\theta_0 - \Delta\theta_n + \omega(\Delta t_n - \Delta t_0)\}] \times \exp[\mathrm{in}(T_R\omega - \phi_{sl})]. \tag{17}$$

To evaluate the expectation in Eq. (17), we assume that the timing variance, phase variance, and time-phase covariance grow linearly with propagation distance, so that

$$\mathbb{E}[(\Delta\theta_n)^2] = C_{\theta\theta}|n|T_R, \qquad \mathbb{E}[(\Delta t_n)^2] = C_{tt}|n|T_R, \tag{18}$$

and $\mathbb{E}[\Delta t_n \Delta\theta_n] = C_{t\theta}|n|T_R$, where the coefficients $C_{\theta\theta}$, C_{tt}, and $C_{t\theta}$ can be computed using Monte Carlo simulations. Next, if we assume that the multivariate random variable $(\Delta\theta_n, \Delta t_n)$ follows a multivariate normal distribution, then the expectation $\mathbb{E}[\exp\{i(\Delta t_n\omega - \Delta\theta_n)\}]$ is the Fourier transform (characteristic function) of a two-dimensional Gaussian, and so [33]

$$S(\omega) = \frac{E}{T_R} |\widehat{U}(\omega)|^2 \sum_{n=-\infty}^{\infty} \exp[-L(\omega)|n|T_R/2 + in(T_R\omega - \phi_{sl})], \tag{19}$$

where the optical comb linewidth function is given by

$$L(\omega) = C_{\theta\theta} - 2C_{t\theta}\omega + C_{tt}\omega^2. \tag{20}$$

After summing a geometric series, we find that

$$S(\omega) = \frac{E}{T_R} |\widehat{U}(\omega)|^2 \times \frac{1 - \exp[-L(\omega)T_R]}{1 - 2\exp[-L(\omega)T_R/2]\cos(T_R\omega - \phi_{sl}) + \exp[-L(\omega)T_R]}. \tag{21}$$

We observe that, except for the ω dependence of L, the final factor in Eq. (21) is the transfer function of a Fabry–Perot filter. The power spectral density, S, therefore consists of a comb of spectral lines with spacing $f_{rep} = 1/T_R$ that is modulated by $(E/T_R)|\widehat{U}(\omega)|^2$. Since $L(\omega)T_R$ is typically small, the shape of the line at frequency ω is well approximated by a Lorentzian function with a full width at half-maximum, FWHM $= L(\omega)/(2\pi)$ Hz. Equation (20) is consistent with the picture of Telle *et al.* [10] in which an elastic tape marked with equally spaced spectral lines is randomly stretched while it is held fixed at a characteristic frequency, ω_{fix}. Therefore, the fluctuations in the line at frequency ω should increase as $|\omega - \omega_{fix}|$ increases. Using this picture, Newbury and Swann [9] provided a physically motivated formula for the linewidth due to ASE noise in a solitonic laser that—like Eq. (20)—has a quadratic dependence on the frequency of the line.

5. NUMERICAL IMPLEMENTATION

We used an evolutionary approach to determine periodically stationary solutions, compute pulse dynamics, determine laser stability, and quantify the noise performance of the laser [6]. We solved Eq. (1) using a modified split-step Fourier method [34] with absorbing boundary conditions. To find periodically stationary solutions, we propagated an initial Gaussian pulse for a large number of round trips of the laser and identified those system parameter regimes for which there was a sufficiently small mean-square error between the solution at 80 and 100 round trips of the laser. To determine the noise performance of the laser, the resulting periodically stationary pulse solution was that used as the initial condition in a Monte Carlo simulation. To study the effects that nonlinear interactions between the pulse and ASE noise have on the noise performance of the laser, we added white Gaussian noise to the pulse each time it passed through the optical fiber amplifier. To obtain sufficiently accurate results, we artificially increased the noise power by a factor of between 10 and 10^4 and then rescaled the results accordingly [7]. We then computed the induced shifts in the pulse parameters at the output coupler, and we quantified the uncertainty in their statistics using confidence intervals calculated from ensembles of Monte Carlo simulations and Student's t distribution [33]. We verified the correctness of our computational method by comparison to analytical results obtained using soliton perturbation theory [6,26,35].

6. RESULTS

We present results for three laser systems: A, B, and C. The baseline System A is closely related to the similariton Yb-fiber laser of Hartl *et al.* [17], although it also includes a narrowband optical filter to ensure the existence of stable pulses when the round-trip dispersion is zero. For System A, we used a fiber amplifier of length $L = 2$ m with a normal dispersion of $\beta = 25$ kfs^2 (1 kfs$^2 = 10^{-27}$ s^2), a nonlinear Kerr coefficient of $\gamma = 0.0044$ (Wm)$^{-1}$, and an amplifier bandwidth of $\Omega_g = 50$ THz. The unsaturated gain was $g_0 = 7$ m^{-1}, and the saturation energy was $E_{sat} = 170$ pJ. The unsaturated loss of the saturable absorber was $l_0 = 0.95$, and the saturation power was $P_{sat} = 1400$ W. We used a Gaussian optical filter with a full width at half-maximum of FWHM $= 1.2$ THz (which corresponds to 4 nm at 1000 nm). The bandwidth of the optical filter was therefore considerably narrower than

that of the fiber amplifier. We adjusted the dispersion of the delay line to vary the round-trip dispersion from $\beta_{RT} = -100$ kfs^2 to $\beta_{RT} = 100$ kfs^2 in increments of 10 kfs^2. Although such a wide range of dispersion values is unlikely to be realized in experimental systems, it is useful to illustrate trends in the pulse dynamics and noise performance. For simulations with noise, we used a spontaneous emission factor of $n_{sp} = 1$ in the fiber amplifier. For computation of comb linewidths, we assumed a round-trip time of $T_R = 10$ ns. The parameters for Systems B and C were the same as those for System A, except that for System B we quadrupled the unsaturated gain of the fiber amplifier to be $g_0 = 28$ m^{-1}, and for System C we doubled the width of the Gaussian optical filter to be FWHM = 2.4 THz.

In Fig. 1, with the solid curves we show plots of the optical power (top row) and local frequency (bottom row) of the pulse at the exit to the fiber amplifier for large negative dispersion ($\beta_{RT} = -50$ kfs^2, left column), small positive dispersion ($\beta_{RT} = 10$ kfs^2, middle column), and large positive dispersion ($\beta_{RT} = 50$ kfs^2, right column). We first assess how close the pulse is to a similariton. In the top row of Fig. 1, we show with a dashed curve the pulse with parabolic power profile, P, that has the same energy, central time, and root mean square (RMS) pulse width as the pulse, u, exiting the fiber amplifier. The agreement is best with Systems A and C at small positive dispersion. In these two cases, the local frequency is also closest to being linear across the pulse. The agreement is also good for System A at large negative and at large positive dispersion, although in these cases the local frequency is not as linear near the edges of the pulse. On the other hand, for System C, the pulse is closer to a Gaussian at large positive dispersion and develops oscillations at large negative dispersion. In fact, for System C at the even larger negative dispersion of $\beta_{RT} = -100$ kfs^2, the solution we found was not periodically stationary. Therefore, we have omitted this dispersion value in subsequent figures that show the pulse dynamics and noise performance of System C.

To further quantify these trends, in Fig. 2 (left), we plot the relative mean-square error, $\mathcal{E}$, between the pulse, u, and the best-fit parabola, P, as a function of β_{RT}. Here we set $\mathcal{E} = \int[|u(t)|^2 - P(t)]^2 dt / \int P(t)^2 dt$, where the integrals are taken over the interval where $P(t) > 0$. Although the error $\mathcal{E}$ is smallest with System C at small positive dispersion, the fit becomes significantly worse as $|\beta_{RT}|$ increases, since the non-parabolic sides of the pulse are not cut off as much by the wider filter (see Fig. 1). On the other hand, the pulse in System A is close to being parabolic when $|\beta_{RT}| < 50$ kfs^2. Comparing the results for Systems A and B, we see that the degree to which the pulse is parabolic depends on having the correct balance between nonlinearity and dispersion. In a wide interval about zero dispersion, the fit is better for System A, whereas at large negative dispersion, the fit is better for System B.

In Fig. 2 (middle), we plot the width of the dechirped pulse at the exit to the system as a function of the round-trip dispersion, β_{RT}. For Systems A, B, and C, the smallest pulse widths are 105 fs at $\beta_{RT} = 0$ kfs^2, 52 fs at $\beta_{RT} = 20$ kfs^2, and 81 fs at $\beta_{RT} = 0$ kfs^2, respectively. For Systems A and B, the pulse widths are less than 140 fs and 70 fs, respectively,

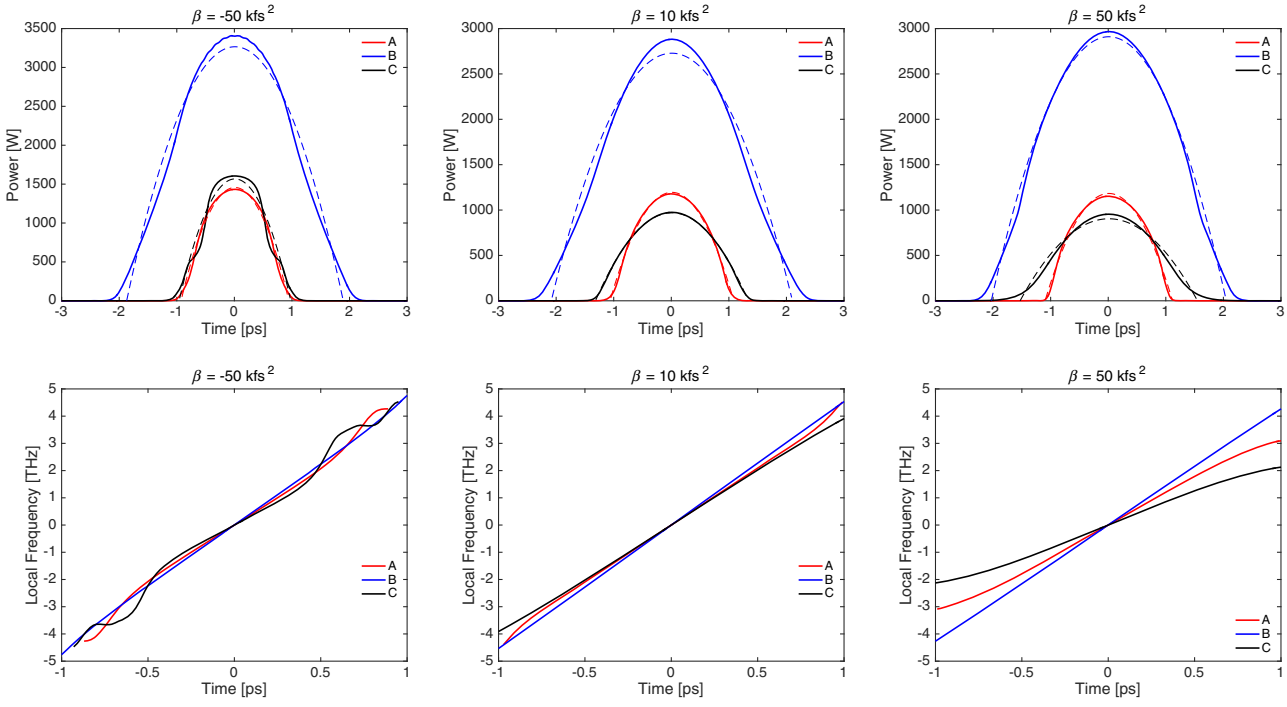

Fig. 1. Optical pulse at the exit to the fiber amplifier. In the top row, we show the pulse power, and in the bottom row we show the local frequency, both as functions of time. (In the bottom row, the time window is one-third of that in the top row.) In the different columns, we show the results for different values of the round-trip dispersion: $\beta_{RT} = -50$ kfs^2 (left), $\beta_{RT} = 10$ kfs^2 (middle), and $\beta_{RT} = 50$ kfs^2 (right). The results for Systems A, B, and C are shown in red, blue, and black, respectively. The dotted curves in the top row show parabolic fits to the pulse power with the same energy and pulse width.

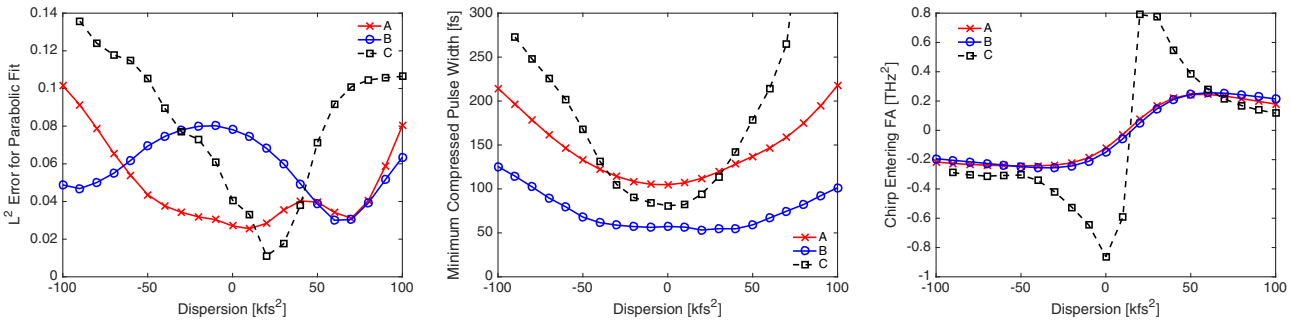

Fig. 2. Left, relative error between the pulse at the exit to the fiber amplifier and the best-fit parabolic pulse as a function of β_{RT}; middle, minimum pulse width after pulse compression at the exit to the laser system as a function of β_{RT}; right, chirp at entrance to fiber amplifier. The results for Systems A, B, and C are shown with red crosses, blue circles, and black squares, respectively.

when $|\beta_{RT}| < 50$ kfs^2. These results corroborate those of Renninger *et al.* [20] that the pulse width in a similariton laser is largely independent of the round-trip dispersion. On the other hand, for System C, the pulse width increases more rapidly as $|\beta_{RT}|$ increases.

In Fig. 3, we plot the RMS pulse width, peak power, and RMS spectral width as functions of the round-trip dispersion, β_{RT}, at the entrance (top row) and exit (bottom row) of the fiber amplifier. In Fig. 2 (right), we plot the chirp at the exit to the fiber amplifier, which crosses zero near the minimally compressed pulse width, and which behaves quite differently for the wide-filter System C than for Systems A and B. For all three systems, the pulse width at the entrance to the fiber amplifier is minimized at small positive dispersion ($\beta_{RT} = 10$ kfs^2), and at that dispersion value, it is smallest for System C. However, for System C the pulse parameters are more sensitive to variations in β_{RT} than is the case for Systems A and B.

For all three systems, the pulse dynamics are closest to that of a similariton when the round-trip dispersion is close to zero. In particular, the energy gain in the fiber amplifier (not shown) is largest near zero dispersion, and ranges between a factor of 25 and 44 for System A, 18 and 41 for System B, and 11 and 36 for System C as the dispersion varies. In addition, the pulse width and spectral width both increase by factors of between 3 and 8 in the fiber amplifier. In particular, the pulse width at the entrance to the fiber amplifier is smallest when the round-trip dispersion is small and positive ($\beta_{RT} \approx 0$ – 20 kfs^2), which results in greater nonlinear spectral broadening in the fiber amplifier. As a consequence, more of the pulse spectrum is cut out by the narrowband optical filter, and so the input energy to the fiber amplifier is also smallest in this dispersion range.

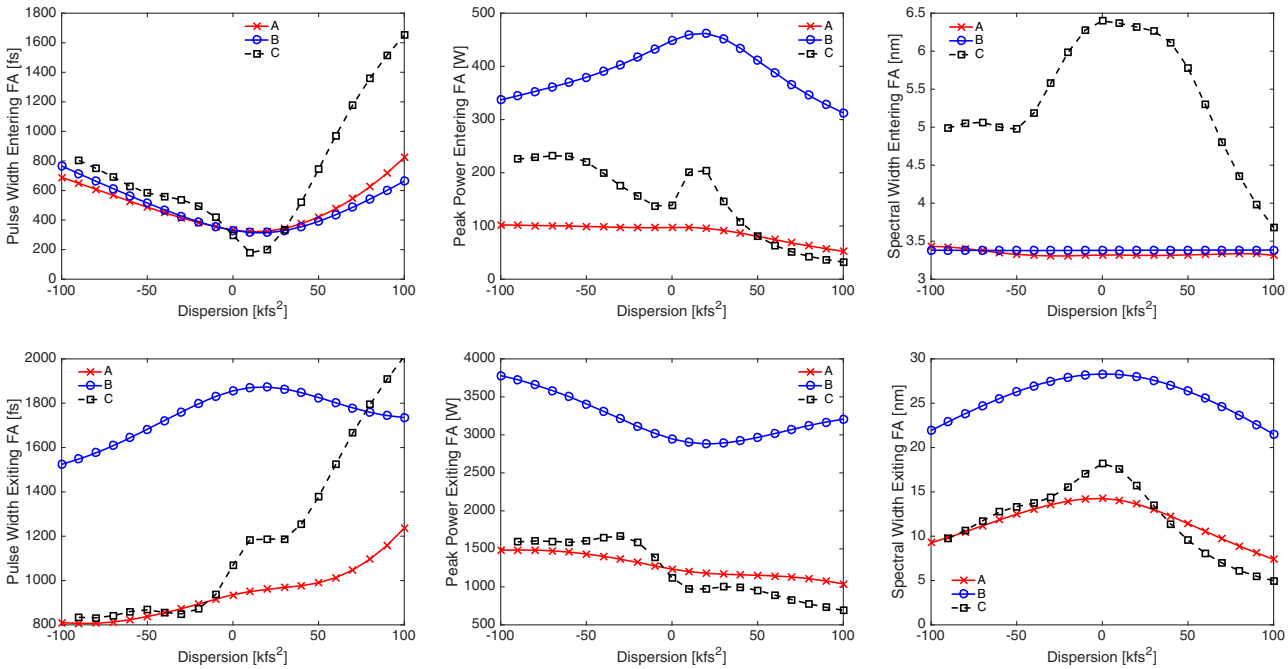

Fig. 3. Pulse parameters as functions of round-trip dispersion, β_{RT}, at the entrance (top row) and exit (bottom row) of the fiber amplifier. Left to right: RMS pulse width, peak power, and RMS spectral width.

In addition, for Systems A and C, the pulse is closest to being parabolic in this same small positive dispersion interval. These pulse dynamics are consistent with that expected of a fiber laser operating in the similariton regime. However, the self-similar, asymptotic solution of the nonlinear Schrödinger equation with simple gain found by Fermann *et al.* [15] only provides qualitative insight into the pulse dynamics in similariton lasers due to the gain saturation, finite bandwidth, and relatively short length of the fiber amplifier [2,16,18].

For Systems A and B, the greater the magnitude of the round-trip dispersion, the less the pulse parameters increase in the fiber amplifier, and the less the pulse behaves like a similariton. Nevertheless, across the entire 200 kfs^2 dispersion range, there is still a large increase in the spectral width of the pulse in the fiber amplifier by a factor of between 2.5 and 8, which is compensated by the action of the narrowband optical filter.

For System C, with large positive dispersion ($\beta_{RT} \geq 60$ kfs^2), the pulse is only weakly influenced by the optical filter. In this parameter regime, the pulse entering the fiber amplifier has a lower peak power and a much larger pulse width than is the case for Systems A and B. Therefore, the effect of the nonlinearity in the fiber amplifier is weaker. As a consequence, both the pulse width and spectral width only increase by factors of between 1.2 and 1.6 in the fiber amplifier. In addition, as we saw in Figs. 1 and 2, at the exit to the fiber amplifier the pulse is close to a Gaussian and the minimum compressed pulse width is much larger than for the other two systems. In summary, in the positive dispersion regime, the pulse dynamics for System C appear to be closer to that of a stretched-pulse laser [25] than to that of a similariton laser.

We now examine the noise performance of the three systems. In the top row of Fig. 4, we plot the frequency jitter (left) and energy jitter (middle) as functions of the round-trip dispersion, β_{RT}. Both quantities are constant as a function of the number of round trips, which is to be expected since the narrowband optical filter stabilizes the frequency, and the gain saturation in the fiber amplifier stabilizes the energy. However, both jitters vary as a function of β_{RT}. This variation is not due to statistical error, since the width of the confidence intervals (not shown) is on the order of 5% of the mean jitter values, and since the jitter plots are independent of the degree of artificial noise scaling (see Section 5). The frequency jitter is smaller for System B than for System A, since for System B the pulse spectrum at the exit to the fiber amplifier occupies more of the available bandwidth of the optical filter (see Fig. 3). Consequently, the optical filter better stabilizes the central frequency of the pulse in the case of System B than in the case of System A. When $\beta_{RT} < -20$ kfs^2, the frequency jitter is the same for Systems A and C. However, for $\beta_{RT} > 0$, the frequency jitter is about 3 times larger for System C than for System A. We suggest that the larger frequency jitter of System C when $\beta_{RT} > 0$ may be due to differences in the pulse parameters of Systems A and C. Specifically, as we see in the bottom row of Fig. 3, at the exit to the fiber amplifier as the dispersion increases from zero, the pulse width tends to increase more rapidly, and the peak power and spectral width tend to decrease more rapidly for System C than for System A.

Next, we consider the timing and phase variance, which we found both increase linearly as a function of the number of round trips. Therefore, in the bottom row of Fig. 4, we plot the timing jitter (left) and phase jitter (middle) per round trip

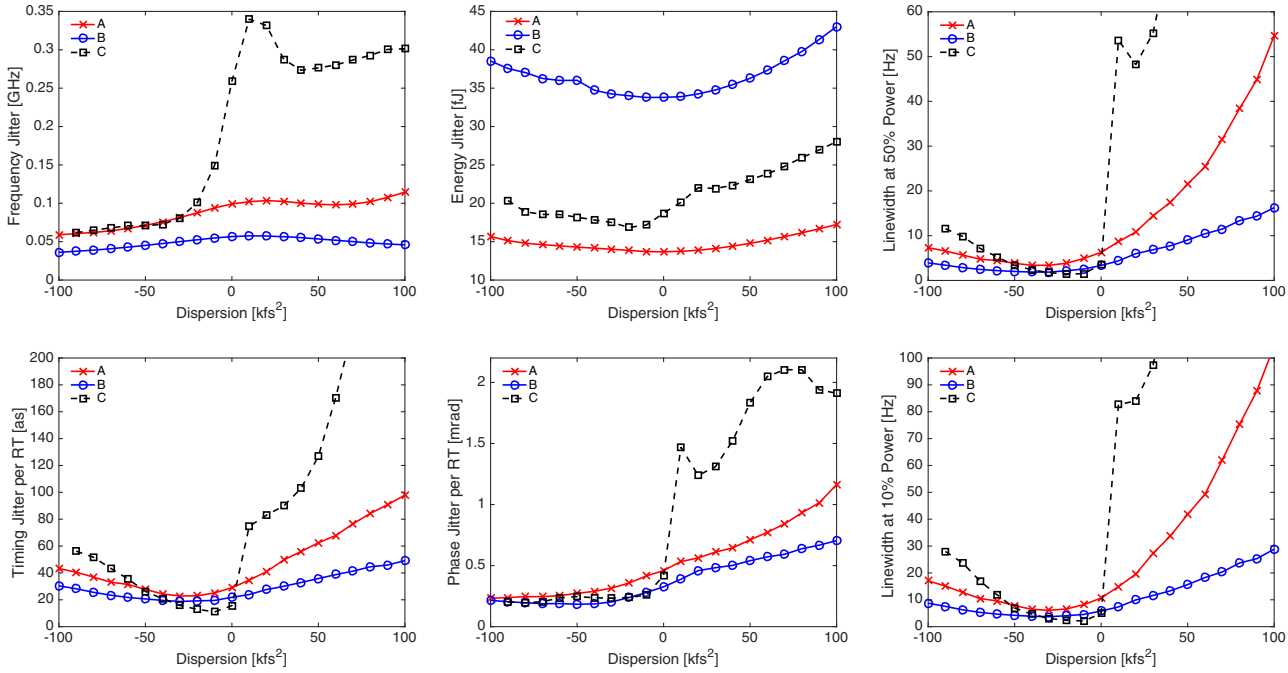

Fig. 4. Jitter and comb linewidths as functions of the round-trip dispersion, β_{RT}. Left column, frequency jitter (top) and timing jitter per round trip (bottom); middle column, energy jitter (top) and phase jitter per round trip (bottom); right column, optical linewidth as a function of the round-trip dispersion, β_{RT}, for the comb lines at the frequency for which the power is 50% (top) and 10% (bottom) of the maximum spectral power for System A at zero dispersion.

as functions of β_{RT}. We recall that these jitters equal the square roots of the corresponding variances. Once again, the width of the confidence intervals (not shown) is on the order of 5% of the mean jitter values. In addition, we used hypothesis testing to conclude that the time-phase covariance is zero.

In both experiments and theory, it is common practice to plot the timing jitter spectrum, $S_{\Delta t}$, as a function of frequency, and to report values, σ_{int}, of timing jitter obtained by integrating $S_{\Delta t}$ over a specified frequency interval, $[f_{\min}, f_{\max}]$. Here we report values of the timing jitter per round trip, $\sigma_{\Delta t}$, which is related to the integrated timing jitter by the formula $\sigma_{\Delta t} = 2\pi[f_{\min} T_R]^{1/2}\sigma_{\text{int}}$ [4]. For the results reported in this paper, we use $f_{\min} = 10$ kHz and $T_R = 10$ ns, so that $\sigma_{\text{int}} = 15.9\sigma_{\Delta t}$.

For the results in Fig. 4, the minimum timing jitter per round trip is $\sigma_{\Delta t} = 11$ as, which occurs for System C at $\beta_{RT} = -10$ kfs^2 and corresponds to an integrated timing jitter of $\sigma_{\text{int}} = 175$ as. For Systems A and B, the minimum timing jitter per round trip is $\sigma_{\Delta t} = 23$ as and 19 as, respectively, both at $\beta_{RT} = -30$ kfs^2. For System C, although $\sigma_{\Delta t} < 25$ as when -40 kfs$^2 < \beta_{RT} < 0$, the timing jitter increases very rapidly as β_{RT} increases from zero, reaching 415 as when $\beta_{RT} = 100$ kfs^2. By comparison, for Systems A and B, the timing jitter is much less sensitive to the round-trip dispersion, especially for System B for which $\sigma_{\Delta t} < 50$ as over the entire dispersion range. Similar trends hold for the phase jitter, with the minimum phase jitter per round trip being 0.184 mrad for System B at $\beta_{RT} = -50$ kfs^2. However, for System C, the phase jitter function has a complicated structure with several local optima that are not due to statistical fluctuations. Motivated by the analysis of timing jitter in a stretched-pulse laser by Namiki and Haus [25], we suggest that the complexity of this structure is due to different phase-shift mechanisms dominating in different dispersion regimes.

Finally, we examine the optical linewidth as a function of the dispersion at three representative frequencies. For these results, we used Eq. (20) to calculate the linewidths in terms of the numerically computed values of the phase and timing variance. First, by Eq. (20), the linewidth at the central frequency is proportional to the phase variance per round trip and has a minimum value of 0.54 Hz with System B at $\beta_{RT} = -50$ kfs^2. (The phase jitter—which is the square root of the phase variance—is shown in the middle of the bottom row of Fig. 4.) Next, in the right column of Fig. 4, we plot the linewidth as a function of the round-trip dispersion, β_{RT}, for the comb lines at the frequencies for which the power is 50% (top) and 10% (bottom) of the maximum spectral power for System A when $\beta_{RT} = 0$. At 50% power, the minimum linewidths are 3.4 Hz for System A at -40 kfs^2, 1.9 Hz for System B at -30 kfs^2, and 1.5 Hz for System C at -10 kfs^2. At 10% power, they are 6.1 Hz for System A at -30 kfs^2, 3.75 Hz for System B at -30 kfs^2, and 2.1 Hz for System C at -10 kfs^2. Just as for the phase and timing jitter, we find that the linewidth is smallest (or close to smallest) for System B, whereas for System C, it increases rapidly as the dispersion increases from zero.

7. DISCUSSION

There are experimental studies of timing jitter in Yb-fiber lasers that show trends similar to our results, and which have been explained using the Namiki–Haus theory for timing jitter in a stretched-pulse fiber laser [25]. However, we are not aware of any prior studies—theoretical or experimental—on the phase jitter in nonsolitonic, passively modulated fiber lasers. While there have been experimental studies of the comb linewidths in nonsolitonic lasers [13,14,36], we know of no prior theoretical or computational studies valid for periodically stationary pulses with large changes each round trip. Significantly, our optical linewidth results are consistent with prior experimental ceo-linewidth results of Nugent-Glandorf *et al.* [14] and of Wise [36].

The timing jitter for System C, which has the wider optical filter, shares some qualitative properties with theoretical results obtained by Namiki and Haus [25] for stretched-pulse lasers. In such lasers, a periodically stationary, chirped Gaussian pulse circulates in a loop consisting of two segments of nonlinear fiber, with opposite signs of dispersion. As a result, the pulse is periodically stretched and recompressed each round trip. This mechanism for pulse breathing is very different from that in a similariton laser, where the pulse width first increases exponentially due to the strong nonlinearity in the fiber amplifier and is then instantaneously decreased by the narrowband optical filter. Despite the different pulse shaping mechanisms, we will show that there are strong similarities in the behavior of the timing jitter in stretched-pulse lasers and in similariton lasers, especially those with wider optical filters. Two of the main results of Namiki and Haus are a formula for the pulse chirp in terms of the system parameters and a formula for the timing jitter as a function of the system parameters and the pulse chirp. They show that the chirp is close to zero for negative dispersion, is small and negative at zero dispersion, and decreases as the dispersion increases above zero. In the negative dispersion regime, this behavior is similar to the results we obtained in Fig. 2 (right) for the chirp at the entrance to the fiber amplifier, although the trends are quite different in the positive dispersion regime. They also study the dependence of the timing jitter on the round-trip dispersion and obtain a hockey-stick-shaped curve that is similar to the timing jitter we obtained for System C in Fig. 4. Their theory shows that there are two main sources of timing shifts: those due to the dispersion-induced conversion of frequency-to-time shifts, and those due to the optical filtering of a chirped pulse. Moreover, they show that a larger pulse width leads to a larger timing jitter, and that if the chirp is nonzero at zero dispersion, then the minimum timing jitter occurs at small negative dispersion rather than at zero dispersion. These results are all consistent with the results in Fig. 4, especially for System C. Moreover, different terms in their formula for the timing jitter can dominate in different dispersion regimes. Therefore, depending on the system parameters, there is the potential for large changes in the slope of the timing jitter curves as the dispersion increases from negative to positive dispersion. Indeed, this phenomenon can be observed in the timing jitter plots for System C in Fig. 4. We suggest that a further development of the Namiki–Haus stretched-pulse theory, or a related theory specific to similariton lasers, could also provide qualitative explanations for the frequency and phase jitter plots shown in Fig. 4.

Our results are also consistent with several experimental studies of timing jitter. Song *et al.* [21] measured timing jitter

spectra for a Yb-fiber laser operating in the soliton, stretched-pulse, and similariton regimes. This system did not include a narrowband optical filter. As the round-trip dispersion increased from −4 to 0 to +3 kfs^2, the integrated timing jitter first decreased slightly from 230 as (16 as per round trip) to 175 as (12 as per round trip) and then increased dramatically to 1,100 as (74 as per round trip). In a second paper, Song *et al.* [22] measured timing jitter spectra of a stretched-pulse Yb-fiber laser for several values of the round-trip dispersion. They found that the timing jitter was smallest at zero dispersion, only slightly larger at small negative dispersion, but was significantly larger at small positive dispersion. For an Er-fiber laser, Kim *et al.* [37] obtained a minimum integrated timing jitter of 70 as (corresponding to 5 as per round trip) when the round-trip dispersion was −2 kfs^2. They also showed that the timing jitter predicted by the Namiki–Haus model for their system was 3–6 times smaller than the measured value.

Two approaches have been explored to reduce the timing jitter in a fiber laser. By inserting a 7 nm optical filter into a loop with a round-trip dispersion of +8 kfs^2, Qin *et al.* [23] reduced the integrated timing jitter by a factor of 12 to 57 as. They also showed that with an optical filter, the timing jitter is less dependent on the dispersion than without it. These results are consistent with the smaller timing jitter and timing jitter slope we observe in the positive dispersion regime for System A, which has a narrower optical filter than System C. More recently, by shortening the length of the nongain fiber and using a round-trip dispersion between −2 and 0 kfs^2, Kim *et al.* [24], obtained a record-low integrated timing jitter for a Yb-fiber laser of 14.3 as, which is comparable to the performance of the lowest timing jitter Ti:sapphire solid-state lasers.

The simulation results that we obtained for the optical comb linewidth as a function of the round-trip dispersion are also consistent with experimental measurements of the ceo linewidths in free-running mode-locked fiber lasers. In experiments, the ceo frequency, f_{ceo}, is measured using the frequency-doubling self-referencing technique of Jones *et al.* [38], in which $f_{\mathrm{ceo}} = 2\nu_n - \nu_{2n}$, where ν_n and ν_{2n} are octave-separated frequencies in the comb. Consequently, the ceo linewidth is related to the widths of optical comb lines near the red and blue ends of the pulse spectrum.

For a Yb-fiber laser without a narrowband filter, Nugent-Glandorf *et al.* [14] studied the dependence of the linewidth of the ceo frequency as a function of the dispersion from $\beta_{\mathrm{RT}} =$ −6 kfs^2 to +11 kfs^2. They found that the ceo linewidth was minimized at zero dispersion, and, as in Fig. 4, that it increases more rapidly as the dispersion increases from zero than when it decreases. In experiments performed using a similariton laser, Wise [36] found that the ceo linewidth decreases at higher pulse energy. This result is consistent with the lower optical linewidths we observe for System B than for System A. In addition, he found that without an optical filter, the ceo linewidth is smallest at zero dispersion, and that it increases more rapidly when the dispersion increases from zero than when it decreases. This trend is the same as that found by Nugent-Glandorf *et al.* [14] and that we observed for optical linewidths with System C (see Fig. 4). However, with an optical filter, Wise found that the ceo linewidth is larger near zero dispersion than without the filter, and increases less rapidly as the magnitude of the dispersion increases, consistent with the results of Qin *et al.* [23] discussed above. Taken together, these trends are similar to those we show in Fig. 4 for Systems C and A.

8. CONCLUSION

For a Yb-fiber laser operating in or near the similariton regime, we used Monte Carlo simulations together with a formula for the optical comb linewidths to compute the jitter in the energy, frequency, timing, and phase of the pulse, and the widths of the lines in the frequency comb, as functions of the round-trip dispersion. Our results provide a more systematic investigation of the parameter space of Yb-laser systems and a more complete description of the noise performance than has so far been obtained in experiments. Over a wide range of dispersion values, the dechirped pulse width, timing jitter, phase jitter, and comb linewidths are smaller at higher average pulse energy. However, over a narrow range of negative dispersion values near zero, the timing jitter and comb linewidths are smaller with a wider optical filter. On the other hand, with the wider optical filter, the pulse width increases significantly, and the noise performance deteriorates rapidly as the dispersion increases above zero. Together with a theoretical study of the timing jitter in a stretched-pulse laser by Namiki and Haus [25], our results provide a partial explanation for the trends in the ceo linewidths that were experimentally measured by Nugent-Glandorf *et al.* [14]. Nevertheless, our work highlights the need for both analytical and computational perturbation theories that can predict and more fully explain the dependence of jitter and comb linewidths on the system parameters, and that are valid for systems in which there are large changes in the pulse parameters each round trip. An outline for such a general computational theory of the stability and noise performance of fiber lasers is given in recent papers of Menyuk and Wang [6] and Shen *et al.* [39].

Acknowledgment. We thank Martin Fermann, William Renninger, Yannan Shen, Shaokang Wang, and Frank Wise for helpful conversations, and the anonymous reviewers for their useful suggestions.

REFERENCES

1. F. Kärtner, U. Morgner, T. Schibli, R. Ell, H. Haus, J. Fujimoto, and E. Ippen, "Few-cycle pulses directly from a laser," in *Few-Cycle Laser Pulse Generation and Its Applications* (Springer, 2004), pp. 73–136.
2. A. Chong, L. G. Wright, and F. W. Wise, "Ultrafast fiber lasers based on self-similar pulse evolution: a review of current progress," Rep. Prog. Phys. **78**, 113901 (2015).
3. A. Chong, W. H. Renninger, and F. W. Wise, "Properties of normal-dispersion femtosecond fiber lasers," J. Opt. Soc. Am. B **25**, 140–148 (2008).
4. H. A. Haus and A. Mecozzi, "Noise of mode-locked lasers," IEEE J. Quantum Electron. **29**, 983–996 (1993).
5. R. Paschotta, "Timing jitter and phase noise of mode-locked fiber lasers," Opt. Express **18**, 5041–5054 (2010).
6. C. R. Menyuk and S. Wang, "Spectral methods for determining the stability and noise performance of passively modelocked lasers," Nanophotonics **5**, 332–350 (2016).
7. R. Paschotta, "Noise of mode-locked lasers (Part I): numerical model," Appl. Phys. B **79**, 153–162 (2004).
8. R. Paschotta, "Noise of mode-locked lasers (Part II): timing jitter and other fluctuations," Appl. Phys. B **79**, 163–173 (2004).

9. N. R. Newbury and W. C. Swann, "Low-noise fiber-laser frequency combs," J. Opt. Soc. Am. B **24**, 1756–1770 (2007).
10. H. R. Telle, B. Lipphardt, and J. Stenger, "Kerr-lens, mode-locked lasers as transfer oscillators for optical frequency measurements," Appl. Phys. B **74**, 1–6 (2002).
11. N. R. Newbury and B. R. Washburn, "Theory of the frequency comb output from a femtosecond fiber laser," IEEE J. Quantum Electron. **41**, 1388–1402 (2005).
12. R. Paschotta, A. Schlatter, S. Zeller, H. Telle, and U. Keller, "Optical phase noise and carrier-envelope offset noise of mode-locked lasers," Appl. Phys. B **82**, 265–273 (2006).
13. J. Wahlstrand, J. Willits, C. Menyuk, and S. Cundiff, "The quantum-limited comb lineshape of a mode-locked laser: fundamental limits on frequency uncertainty," Opt. Express **16**, 18624–18630 (2008).
14. L. Nugent-Glandorf, T. A. Johnson, Y. Kobayashi, and S. A. Diddmans, "Impact of dispersion on amplitude and frequency noise in a Yb-fiber laser comb," Opt. Lett. **36**, 1578–1580 (2011).
15. M. Fermann, V. Kruglov, B. Thomsen, J. Dudley, and J. Harvey, "Self-similar propagation and amplification of parabolic pulses in optical fibers," Phys. Rev. Lett. **84**, 6010–6013 (2000).
16. F. Ilday, J. Buckley, W. Clark, and F. Wise, "Self-similar evolution of parabolic pulses in a laser," Phys. Rev. Lett. **92**, 213902 (2004).
17. I. Hartl, T. Schibli, A. Marcinkevicius, D. Yost, D. Hudson, M. Fermann, and J. Ye, "Cavity-enhanced similariton Yb-fiber laser frequency comb: 3×10^{14} W/cm^2 peak intensity at 136 MHz," Opt. Lett. **32**, 2870–2872 (2007).
18. B. G. Bale and S. Wabnitz, "Strong spectral filtering for a mode-locked similariton fiber laser," Opt. Lett. **35**, 2466–2468 (2010).
19. W. H. Renninger, A. Chong, and F. W. Wise, "Self-similar pulse evolution in an all-normal-dispersion laser," Phys. Rev. A **82**, 021805 (2010).
20. W. H. Renninger, A. Chong, and F. W. Wise, "Amplifier similaritons in a dispersion-mapped fiber laser [invited]," Opt. Express **19**, 22496–22501 (2011).
21. Y. Song, K. Jung, and J. Kim, "Impact of pulse dynamics on timing jitter in mode-locked fiber lasers," Opt. Lett. **36**, 1761–1763 (2011).
22. Y. Song, C. Kim, K. Jung, H. Kim, and J. Kim, "Timing jitter optimization of mode-locked Yb-fiber lasers toward the attosecond regime," Opt. Express **19**, 14518–14525 (2011).
23. P. Qin, Y. Song, H. Kim, J. Shin, D. Kwon, M. Hu, C. Wang, and J. Kim, "Reduction of timing jitter and intensity noise in normal-dispersion passively mode-locked fiber lasers by narrow band-pass filtering," Opt. Express **22**, 28276–28283 (2014).
24. H. Kim, P. Qin, Y. Song, H. Yang, J. Shin, C. Kim, K. Jung, C. Wang, and J. Kim, "Sub-20-attosecond timing jitter mode-locked fiber lasers," IEEE J. Sel. Top. Quantum Electron. **20**, 260–267 (2014).
25. S. Namiki and H. A. Haus, "Noise of the stretched pulse fiber laser. I. Theory," IEEE J. Quantum Electron. **33**, 649–659 (1997).
26. C. McKinstrie and C. Xie, "Phase jitter in single-channel soliton systems with constant dispersion," IEEE J. Sel. Top. Quantum Electron. **8**, 616–625 (2002).
27. T. Schibli, I. Hartl, D. Yost, M. Martin, A. Marcinkevičius, M. Fermann, and J. Ye, "Optical frequency comb with submillihertz linewidth and more than 10 W average power," Nat. Photonics **2**, 355–359 (2008).
28. P. Li, W. H. Renninger, Z. Zhao, Z. Zhang, and F. W. Wise, "Frequency noise of amplifier-similariton laser combs," in *CLEO: Science and Innovations* (Optical Society of America, 2013), paper CTu1I.6.
29. W. Chen, Y. Song, K. Jung, M. Hu, C. Wang, and J. Kim, "Few-femtosecond timing jitter from a picosecond all-polarization-maintaining Yb-fiber laser," Opt. Express **24**, 1347–1357 (2016).
30. G. P. Agrawal, *Nonlinear Fiber Optics* (Academic, 2007).
31. E. Iannone, F. Matera, A. Mecozzi, and M. Settembre, *Nonlinear Optical Communication Networks* (Wiley, 1998).
32. R. O. Moore, G. Biondini, and W. L. Kath, "A method to compute statistics of large, noise-induced perturbations of nonlinear Schrödinger solitons," SIAM Rev. **50**, 523–549 (2008).
33. A. Papoulis and S. U. Pillai, *Probability, Random Variables, and Stochastic Processes* (McGraw-Hill, 2002).
34. S. Wang, A. Docherty, B. Marks, and C. Menyuk, "Comparison of numerical methods for modeling laser mode locking with saturable gain," J. Opt. Soc. Am. B **30**, 3064–3074 (2013).
35. H. A. Haus, "Quantum noise in a solitonlike repeater system," J. Opt. Soc. Am. B **8**, 1122–1126 (1991).
36. F. Wise, personal communication (Cornell University, 2016).
37. T. K. Kim, Y. Song, K. Jung, C. Kim, H. Kim, C. H. Nam, and J. Kim, "Sub-100-as timing jitter optical pulse trains from mode-locked Er-fiber lasers," Opt. Lett. **36**, 4443–4445 (2011).
38. D. Jones, S. Diddams, J. Ranka, A. Stentz, R. Windeler, J. Hall, and S. Cundiff, "Carrier-envelope phase control of femtosecond mode-locked lasers and direct optical frequency synthesis," Science **288**, 635–639 (2000).
39. Y. Shen, J. Zweck, S. Wang, and C. Menyuk, "Spectra of short pulse solutions of the cubic-quintic complex Ginzburg Landau equation near zero dispersion," Stud. Appl. Math. **137**, 238–255 (2016).

130.65.94.108 {ts '2018-04-26 13:57:15'}